Fermionic Light in Common Optical Media

David Novoa, Humberto Michinel, and Daniele Tommasini

Departamento de Física Aplicada, Facultade de Ciencias de Ourense, Universidade de Vigo, As Lagoas s/n, Ourense, ES-32004 Spain

(Received 29 July 2010; published 12 November 2010)

Recent experiments have proved that the response to short laser pulses of common optical media, such as air or oxygen, can be described by focusing Kerr and higher order nonlinearities of alternating signs. Such media support the propagation of steady solitary waves. We argue by both numerical and analytical computations that the low-power fundamental bright solitons satisfy an equation of state which is similar to that of a degenerate gas of fermions at zero temperature. Considering, in particular, the propagation in both O_2 and air, we also find that the high-power solutions behave like droplets of ordinary liquids. We then show how a grid of the fermionic light bubbles can be generated and forced to merge in a liquid droplet. This leads us to propose a set of experiments aimed at the production of both the fermionic and liquid phases of light, and at the demonstration of the transition from the former to the latter.

DOI: 10.1103/PhysRevLett.105.203904 PACS numbers: 42.65.Tg, 03.75.Ss, 42.62.−b, 42.65.Jx

In suitable optical media, light has been argued to acquire material properties. A long-known example is the equivalence of the paraxial propagation of a laser pulse in a Kerr medium with the time evolution of a superfluid Bose-Einstein condensate, due to the identity of the nonlinear Schrödinger equation with the Gross-Pitaevskii equation [1]. More recently, optical induction has been used to create photonic crystals [2], a photonic system has been designed that may undergo a Mott insulator to superfluid quantum phase transition [3], and soliton solutions for light propagation in cubic-quintic (CQ) nonlinear media have been shown to behave like ordinary liquids [4,5].

On the other hand, recent experimental and theoretical works have proved that the response to ultrashort laser pulses of common optical media, such as air or oxygen, can be described by focusing Kerr [6] and higher order nonlinearities of alternating signs [7], which have also been argued to provide the main mechanism in filament stabilization, instead of the plasma defocusing [7].

In this Letter, we demonstrate by analytical and numerical computations that such media can support the propagation of steady solitary waves that appear in two clearly different phases. The low-power solitons are governed by the same equation of state as a degenerate gas of fermions. We will call such a system "fermionic light." On the other hand, the high-power localized states satisfy the Young-Laplace (YL) equation that governs the formation of droplets in ordinary liquids, similarly to the result that was recently obtained for the CQ model [5]. We also show how to generate a grid of fermionic light bubbles and make it turn into a liquid light droplet.

We will consider the (paraxial) propagation along the z direction of a linearly polarized laser beam, so that the complex electric field component $\Psi(x, y, z)$ satisfies the nonlinear Schrödinger equation

$$i\frac{\partial\Psi}{\partial z} + \frac{1}{2k_0 n_0}\nabla_\perp^2\Psi + k_0\Delta n\Psi = 0, \tag{1}$$

where n_0 is the linear refractive index of the medium, $\nabla_\perp^2 = \partial^2/\partial x^2 + \partial^2/\partial y^2$ is the transverse Laplace operator, and $k_0 = 2\pi/\lambda_0$ is the mean wave number in vacuum, where λ_0 is the central wavelength of the laser source which will be fixed to $\lambda_0 = 800$ nm throughout this Letter as in the experiment of Ref. [7]. For the optical media that have been studied in Ref. [7], the nonlinear correction Δn to the refractive index can be expanded as

$$\Delta n \simeq n_2|\Psi|^2 + n_4|\Psi|^4 + n_6|\Psi|^6 + n_8|\Psi|^8, \tag{2}$$

with alternating sign coefficients $n_2, n_6 > 0$ and $n_4, n_8 < 0$ that contribute to focusing and defocusing, respectively. Taking into account that the values of the second-order dispersion and multiphoton-absorption coefficients for air are $k'' = 0.2\ \mathrm{fs}^2/\mathrm{cm}$ and $\beta = 1.27 \times 10^{-126}\ \mathrm{cm}^{17}/\mathrm{W}^9$ [8], respectively, we have checked that both effects do not lead to significant corrections in our results. To be concrete, we will perform most of the numerical calculations in the case of O_2 as the propagation medium, taking the mean values obtained in the experiment [7], $n_2 = 1.6 \times 10^{-19}\ \mathrm{cm}^2/\mathrm{W}$, $n_4 = -5.2 \times 10^{-33}\ \mathrm{cm}^4/\mathrm{W}^2$, $n_6 = 4.8 \times 10^{-46}\ \mathrm{cm}^6/\mathrm{W}^6$, $n_8 = -2.1 \times 10^{-59}\ \mathrm{cm}^8/\mathrm{W}^4$. For comparison, however, we will also mention the results that we obtain for air, using the corresponding values for the coefficients n_{2q} that are also given in Ref. [7].

We will search for finite localized solutions of Eq. (1) of the form $\Psi(x, y, z) = \Phi(r)e^{-i\mu z}$, where $r = \sqrt{x^2 + y^2}$ and μ is the propagation constant. Figure 1 shows the result of our numerical computation for $\Phi(0)$ in the existence domain of such solitons in oxygen ($\mu_\infty < \mu < 0$), where $\mu_\infty = -0.096\ \mathrm{cm}^{-1}$, and for the radial profiles $\Phi(r)$ of three of them (see left-hand inset in Fig. 1), corresponding to the low-power (black solid line), moderate-power

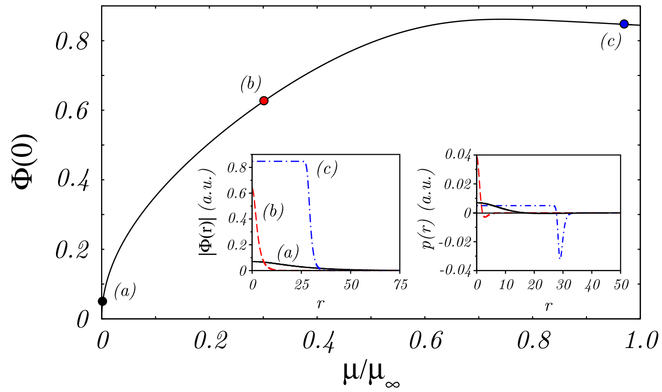

FIG. 1 (color online). Plot of the central amplitude $\Phi(0)$ vs μ/μ_∞ for the family of fundamental eigenstates of Eq. (1). Note that $\Phi(0)$ has a maximum for $\mu/\mu_\infty \approx 0.7$, due to the defocusing nonlinearities. Left-hand inset: Radial profiles of three eigenfunctions of Eq. (1) with $\mu/\mu_\infty = 0.004$ (black solid line), $\mu/\mu_\infty = 0.3$ (red dashed line), and $\mu/\mu_\infty = 0.97$ (blue dash-dotted line), respectively. Right-hand inset: Radial pressure profiles corresponding to these solutions. The low-power profile is magnified by a factor of 10^3 for clarity. Labeled points on the main curve refer to the eigenstates displayed within the insets.

(red dashed line), and high-power regimes (blue dash-dotted line), respectively. We express the transverse spatial variables x, y in terms of the adimensional coordinates ξ, χ, measured in units of $(n_4/n_0)^{1/2}(k_0 n_2)^{-1}$. The amplitude $|\Phi(0)|$ is measured in units of $(n_2/n_4)^{1/2}$.

As in the CQ case, μ can be identified with the chemical potential of an equivalent thermodynamical two-dimensional system [5] of $N = \int \rho dxdy \equiv \int |\Phi|^2 dxdy$ particles, described by the Landau grand potential [9] $\Omega = -\int p dxdy$, where the pressure field p is now

$$p = -\frac{1}{2k_0 n_0}|\nabla_\perp \Phi|^2 + \mu|\Phi|^2 + k_0 \sum_{q=1}^{4} n_{2q}\frac{\Phi^{2(q+1)}}{q+1}. \quad (3)$$

For our optical system, μ, N, Ω, and p correspond to the propagation constant, the power, the Lagrangian leading to Eq. (1), and the Lagrangian density, respectively.

The right-hand inset of Fig. 1 shows the pressure distributions $p(r)$, measured in units of $k_0 n_2^3 n_4^{-2}$, corresponding to the stationary states discussed above. Notice that all the radial distributions display both positive and negative pressure regions, because this a necessary condition for the existence of solitary waves. For the low-power soliton (black solid line), corresponding to small values of $|\mu|$, we can obtain an analytical expression by using the variational method with the ansatz $\Phi(A, r) = A\exp(-r^2/R^2)$. The values of $A(\mu)$ and $R(\mu)$ that minimize Ω for a given value of μ can then be used to compute the pressure distribution. Taking the first nonvanishing order in $|\mu|$ and inverting the dependence $R(\mu)$, we find a simple analytical approximation for the central pressure p_c as a function of either the radius $R = \sqrt{2\langle r^2\rangle}$ of the soliton or the central density $\rho_c = |\Phi(0)|^2$ (corresponding to the beam intensity),

$$p_c = \frac{a}{k_0^3 n_0^2 n_2}\frac{1}{R^4} = b k_0 n_2 \rho_c^2, \quad (4)$$

with $a = 4$ and $b = 1/4$. This relation is similar to the equation of state of a degenerate gas of fermions of mass m at zero temperature. In fact, if we apply the general definition of the Fermi momentum [9] P_F to a two-dimensional system, we obtain $P_F = \hbar\sqrt{2\pi\rho}$, with ρ the density of the Fermi gas. As a consequence, the pressure, defined as the average force on a unit orthogonal line in the gas, can be obtained from the average kinetic energy as follows:

$$p = \rho\langle E_{\mathrm{kin}}\rangle = \frac{\rho}{2m}\frac{\int_0^{P_F} P^2 P dP}{\int_0^{P_F} P dP} = \frac{\pi\hbar^2}{2m}\rho^2, \quad (5)$$

which shows the same dependence with ρ^2 as Eq. (4). This proves the formal analogy of our low-power solitons with a degenerate Fermi gas in the central region around $r = 0$, which is arbitrarily large in the limit $\mu \to 0$ (corresponding to large radius $R \to \infty$). For these reasons, we will call "fermionic" the phase where the pressure is proportional to ρ^2.

Note that in the limit $\mu \to 0$ our variational computation gives a constant $N = \frac{2\pi}{k_0^2 n_0 n_2}$, which is consistent with the known result for the power flow leading to the collapse threshold in a Kerr medium [10]. The magnitude of this power N lies in the range of few GW in both O_2 and air, and can be interpreted as the threshold for the existence of the fermionic light solitons.

Figure 2 shows the numerical computation of p_c as a function of either R (black solid line) or ρ_c (inset, black solid line) for all the nodeless solitary states of the model. The lower branch, corresponding to the low-power solitons, is in excellent agreement with the dependence described by Eq. (4), as it can be inferred from the fitting (red dotted) straight line with slope $s_{\mathrm{low}} = -4$. Furthermore, in the inset of Fig. 2 we also show the quantitative agreement between theory and numerics by comparing p_c with ρ_c instead of R. In this case, the slope of the straight line is $s_{\mathrm{inset}} = 2$, thus demonstrating the quadratic dependence on ρ_c given by Eq. (4). However, the correct numerical values of the constants are $a = 2.5$ and $b = 0.29$, in reasonable agreement with the result of the variational method given above. We have checked numerically that the asymptotic behavior represented by the red lines in Fig. 2 (dotted line and dashed line in the inset) is practically independent of the higher order nonlinearities n_{2q} $(q > 1)$, as predicted by the theory. In particular, these results can be directly applied to both Kerr and CQ models.

On the other hand, the high-power localized solutions exhibit top-flat profiles with an inhomogeneous negative pressure profile on the border, similar to those of the solitons appearing in the CQ model [5]. As a

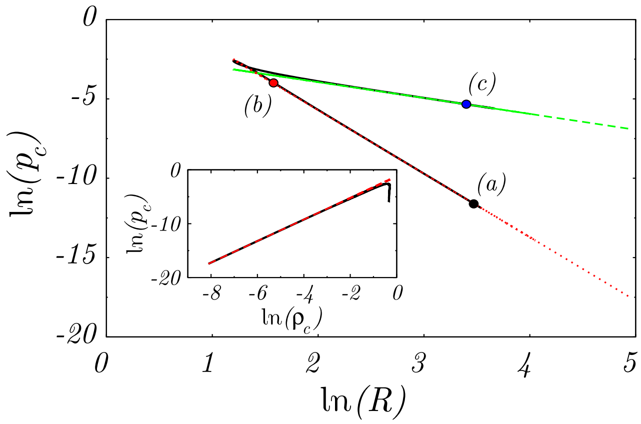

FIG. 2 (color online). Plot of the logarithms of p_c vs R for the fundamental solitons (black line). The fermionic behavior of Eq. (4) (red dotted line) and the liquid YL equation (green dashed line) are compared with the numerics. The labeled points correspond to the same eigenstates displayed in Fig. 1. For each value of R, two different outcomes are possible depending on the power, corresponding to two different phases of light. Inset: Plot of $\ln(p_c)$ vs $\ln(\rho_c)$ (black solid line) overlapped with Eq. (4) (red dashed line) for comparison.

consequence, the gradient term in Eq. (1) can be neglected close to the origin, and we get $\mu = -k_0 \Delta n(0) = -k_0 \sum_{q=1}^{4} n_{2q} \Phi(0)^{2q}$. By generalizing the argument of Ref. [5] including the higher order nonlinearities, we obtain that these states obey the celebrated YL equation [11], $p_c = 2\sigma/R$, describing the behavior of usual liquid droplets. The value of the surface tension is

$$\sigma = \frac{n_2}{\sqrt{2n_0 n_4}} \int_0^{\Phi_\infty} \left(-\mu_\infty \Phi^2 - k_0 \sum_{q=1}^{4} n_{2q} \frac{\Phi^{2(q+1)}}{q+1} \right)^{1/2} d\Phi, \tag{6}$$

where μ_∞ and Φ_∞ are the asymptotic values corresponding to the $R \to \infty$ droplet, which can be computed by solving the equation $p_c = 0$ (neglecting the Laplacian term). For the propagation in oxygen, we have obtained the following variational estimations: $\mu_\infty = -0.247(k_0 n_2^2 n_4^{-1}) = -0.096\ \mathrm{cm}^{-1}$, $\Phi_\infty^2 = 0.712(n_2 n_4^{-1}) = 2.19 \times 10^{13}\ \mathrm{W/cm}^2$, $\sigma = 0.0715(n_2^2 n_4^{-3/2} n_0^{-1/2}) = 4.88 \times 10^9\ \mathrm{W/cm}^2$. These results, obtained assuming a top-flat function, are in excellent agreement with the computation given in Fig. 1. In Fig. 2, we show that our numerical solution in the case of O_2 satisfies the YL equation (green dashed line) with very good accuracy for a wide range of values of μ. On the other hand, for the propagation in air, the liquid light phase would correspond to a higher intensity, $[\Phi_\infty^2]_a = 2.98 \times 10^{13}\ \mathrm{W/cm}^2$, with $[\mu_\infty]_a = -0.116\ \mathrm{cm}^{-1}$ and $[\sigma]_a = 7.16 \times 10^9\ \mathrm{W/cm}^2$, and the YL equation would still be valid.

As we have seen above, the propagation of self-guided light beams in media like oxygen can occur in two clearly separated phases, satisfying two different equations of state. In fact, we have checked that qualitatively similar results can also be obtained for the CQ case, and occur whenever the nonlinear refractive index displays a single well-defined maximum as a function of the intensity. It would then be interesting to demonstrate the possibility of a transition between the fermionic bubbles and the liquid droplets of light. A suggestive analogy is that of the collapse of a star, that occurs when the gravitational interaction overcomes the Fermi pressure of the electrons. We can obtain a qualitatively similar result in the case of light propagation in oxygen, by compressing the fermionic bubbles using a harmonic potential, leading to the generation of a liquid light droplet. Figure 3 shows the result of our simulation in O_2. The initial state (see left-hand snapshot in Fig. 3) consists of a regular grid of fermionic light bubbles with $\mu/\mu_\infty = 0.3$ (see their radial profile in Fig. 1), with a separation between nearest neighbors $\Delta_{\xi,\chi} = 40$. We include an external harmonic potential $V(\xi, \chi) = \frac{K}{2}(\xi^2 + \chi^2)$ with $K = 5 \times 10^{-5}$ in Eq. (1) in order to induce a net force acting on the grid with the aim of making all the fermionic solitons collide in the center of the computational window $(\xi, \chi) = 0$.

This parabolic potential can be obtained by inducing in the medium a "gas lens"[12], which can be constructed with an electrically heated pipe through which passes a laminar flow of gas. By controlling the differential heating at the boundaries and the velocity of the flow, a parabolic

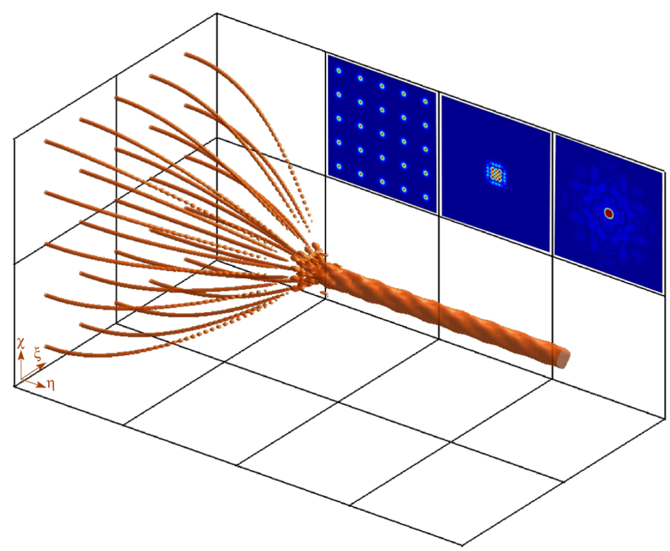

FIG. 3 (color online). Isosurface intensity plot of the dynamical phase transition from a square grid of fermionic light solitons to an individual liquid light soliton in O_2. All solitons in the grid are eigenstates with $\mu/\mu_\infty = 0.3$ displayed in Fig. 1. They are forced to merge in the center of the computational window by means of an external harmonic potential. We can see three pseudocolor plots displaying the initial condition (left, $\eta = 0$), the collapse of the light bubbles (middle, $\eta = 200$), and the final state (right, $\eta = 500$). In the latter we observe a flattop soliton with radius $R \approx 10$ and $\rho_c \approx 0.76$ arising after the massive coalescence of the fermionic solitons. The width of the square spatial domain displayed is $w_{\xi,\chi} = 200$.

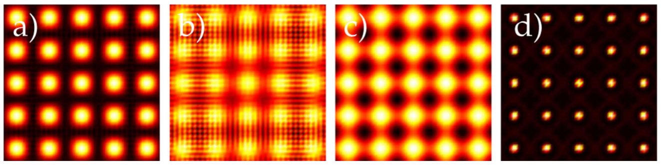

FIG. 4 (color online). Proposal for the generation of the initial condition of Fig. 3 in experimental setups. The (a) pseudocolor plot shows the bidimensional cosine squaredlike phase distribution to be imprinted onto the ingoing beam. We assume that the beam is much wider than the filaments, and restrict our simulation to a square domain $\xi, \chi \in [-75, 75]$ where the wave front is assumed to be homogeneous. In (b),(c) ($\eta = 100, 200$) we observe how the beam profile starts to destabilize, leading to the formation of a grid of spatial solitons at $\eta = 300$ [see (d)].

refractive index gradient can be obtained as documented in Ref. [12]. On the other hand, we have also checked numerically that the same qualitative result can be obtained by using a glass lens, provided that its focal length f is at least 10 times greater than the Rayleigh length of the input beams, which in the case depicted in Fig. 3 corresponds to $f = 5$ m.

For simplicity, we have prepared the initial state with exact solutions of Eq. (1) to reduce the excitation of linear radiative modes. We have checked that such an initial guess can be generated experimentally by means of the modulational instability of a low-power probe pulse. In fact, Fig. 4 shows the results of a numerical simulation where we have added an initial cosine squared-type phase distribution [see Fig. 4(a)] to a homogeneous plane wave in order to excite a regular grid of solitons, as in Ref. [13]. As shown in Figs. 4(b)–4(d), this allows us to control the spatial location of the optical filaments generated during the beam breakup due to modulational instability. The outgoing grid of spatial solitons is depicted in Fig. 4(d). Note its similarity with the initial state of Fig. 3.

Let us come back to the results of Fig. 3. The massive coalescence of all the fermionic bubbles occurs after a finite propagation distance $\eta = 200$ (see middle snapshot in Fig. 3), measured in units of $n_4 k_0^{-1} n_2^{-2}$. As a result, a unique filament structure with large radius arises, as it can be appreciated in Fig. 3. We have checked that this soliton is a flattop eigenstate with radial perturbations coming from the transition process. In fact, we have estimated its logarithmic radius to be around 2.3 and its peak density $\rho_c \approx 0.76$ (measured in units of n_2/n_4, thus corresponding to an intensity 2.34×10^{13} W/cm^2), which is clearly on the liquid light branch displayed in Fig. 2. For oxygen [7], we have considered a propagation distance of about 13 m. Although such a distance seems to be huge for a real experiment, we have verified that by stretching the external potential this distance can be realistically reduced by almost 1 order of magnitude. Finally, we note that the use of pressurized O_2 or air may also help to enhance the nonlinear optical response. For all these reasons, we conclude that the demonstration of the existence of both fermionic and liquid light and the phase transition between them would be an affordable challenge in real experiments.

In conclusion, we have proved that common media (O_2, air) can support the propagation of solitary waves that appear in two clearly different phases with unequal physical properties, namely, the low-power "fermionic" light, satisfying an equation of state similar to that of a degenerate gas of fermions, and the high-power "liquid" light, obeying the YL equation. We have then shown how a grid of the fermionic light bubbles can be generated and forced to merge in a liquid droplet. We think that the possible experimental validation of our proposal could also provide an independent way to corroborate the deep change in the understanding of the filamentation process in gases that was proposed in Ref. [7]. Furthermore, these results in air pave the way for the improvement of recent experiments on laser-induced water condensation [14], built on top of these new robust light distributions.

This work was supported by MICINN, Spain (Project No. FIS2008-01001). D. N. acknowledges support from Consellería de Economía e Industria-Xunta de Galicia through the "Maria Barbeito" program.

[1] *Emergent Nonlinear Phenomena in Bose-Einstein Condensates*, edited by P. G. Kevrekidis, D. J. Frantzeskakis, and R. Carretero-Gonzalez (Springer-Verlag, Berlin, 2008).
[2] T. Pertsch, P. Dannberg, W. Elflein, A. Brauer, and F. Lederer, Phys. Rev. Lett. **83**, 4752 (1999); R. Morandotti, U. Peschel, J. S. Aitchison, H. S. Eisenberg, and Y. Silberberg, Phys. Rev. Lett. **83**, 4756 (1999); H. Martin, E. D. Eugenieva, Z. Chen, and D. N. Christodoulides, Phys. Rev. Lett. **92**, 123902 (2004); B. Freedman *et al.*, Nature (London) **440**, 1166 (2006); T. Schwartz *et al.*, Nature (London) **446**, 52 (2007).
[3] A. D. Greentree, C. Tahan, J. H. Cole, and L. C. L. Hollenberg, Nature Phys. **2**, 856 (2006).
[4] H. Michinel, J. Campo-Taboas, R. Garcia-Fernandez, J. R. Salgueiro, and M. L. Quiroga-Teixeiro, Phys. Rev. E **65**, 066604 (2002).
[5] D. Novoa, H. Michinel, and D. Tommasini, Phys. Rev. Lett. **103**, 023903 (2009).
[6] C. Ruiz *et al.*, Phys. Rev. Lett. **95**, 053905 (2005).
[7] V. Loriot, E. Hertz, O. Faucher, and B. Lavorel, Opt. Express **17**, 13 429 (2009); Opt. Express **18**, 3011(E) (2010); P. Bejot *et al.*, Phys. Rev. Lett. **104**, 103903 (2010).
[8] S. Tzortzakis *et al.*, Phys. Rev. Lett. **86**, 5470 (2001).
[9] L. D. Landau and E. M. Lifshitz, *Statistical Physics* (Pergamon, Oxford, 1984).
[10] J. H. Marburger, Prog. Quantum Electron. **4**, 35 (1975).
[11] J. Eggers, Rev. Mod. Phys. **69**, 865 (1997).
[12] M. Notcutt *et al.*, Opt. Laser Technol. **20**, 243 (1988); M. M. Michaelis *et al.*, Nature (London) **353**, 547 (1991).
[13] H. Schroeder, J. Liu, and S. L. Chin, Opt. Express **12**, 4768 (2004); M. R. Fetterman *et al.*, Opt. Express **3**, 366 (1998).
[14] P. Rohwetter *et al.*, Nat. Photon. **4**, 451 (2010).